



Assessment of Grid Connected PEM Fuel Cell Power System using Matlab/Simulink Stateflow models

Hamza Bahri^{a,b} and Abdelghani Harrag^{a*}

^a*Mechatronics Laboratory (LMETR) - E1746200, Optics and Precision Mechanics Institute, Ferhat Abbas University, Cite Maabouda (ex. Travaux), 19000 Setif, Algeria*

^b*Electrical Engineering Department, Faculty of Technology, Mohamed Boudiaf University, 28000 Msila, Algeria*

ARTICLE INFO

Article history:

Received 07 July 2020

Accepted 04 December 2020

Keywords:

Fuel Cell,
PEMFC,
MPPT,
Variable step size Incremental
Conductance,
Boost,
Inverter

ABSTRACT

This paper addresses the development of three-phase grid connected fuel cell energy system using Matlab/Simulink Stateflow environment. The proposed grid connected fuel energy system designed by considering a 5.5kW proton exchange membrane fuel cell connected to the grid via a double stage including a DC-DC boost converter and three phase inverter. The whole energy system has been implemented using Matlab/Simulink Stateflow environment where all the parameters and operating conditions have been considered. The proposed energy system has been tested and validated using Matlab/Simulink under different test scenario representing different operating conditions. Simulation obtained results prove the efficiency of the developed stateflow models to characterize and analyzing the PEM fuel cell power system as well as the connection to the grid. The developed models can be used as a platform to analyze the performance of the system in connected or unconnected cases.

* Corresponding author, E-mail address: : a.b.harrag@gmail.com

Tel.: +213 796 966 142

ISSN: 1112-2242 / EISSN: 2716-8247



This work is licensed under a Creative Commons Attribution-ShareAlike 4.0 International License.

Based on a work at <http://revue.cder.dz>.

1. Introduction

Carbon dioxide emissions are a concern for the developed world because of their adverse environmental and health impacts. The increase in the world's population and the increase in energy demand pose a problem in increasing harmful emissions from conventional electricity generation. Today; all eyes are on hydrogen energy, part of the chemical composition of water H_2O . Hydrogen is characterized by its lightness, rapid diffusion and combustion. Its burning is a source of energy. Energy is essential to our daily lives and meets the world's growing needs, while reducing carbon dioxide emissions is the crucial issue of our time. When we look at the history of global energy policies, we can clearly notice that a different source is chosen every few decades, reflecting our creative evolution over time [1].

Energy changes with time, and society evolves with it. In January 2017, the World Hydrogen Council, a global initiative to use hydrogen as a new energy, was established with the participation of 13 leading companies in the world in the fields of energy, transport and manufacturing. In September 2018, 53 new companies joined the initiative; many hopes complicate the expansion in the use of hydrogen energy. On 23 October 2018, the first international conference on the prospects for the use of hydrogen gas was held in Tokyo [1].

Fuel cells, more generally, the hydrogen sector is an interesting way to valorize the chemical energy contained in various fuels, with a very good efficiency, in the noble form of electrical energy. There are six fuel cell technologies currently available in the market differ from each other in terms of the chemical nature of the electrolyte, the operating temperature and the choice of fuel [2][3]. These types of fuel cells are: Solid Oxide Fuel Cell (SOFC), Proton Exchange Membrane Fuel Cell (PEMFC), Alkaline Fuel Cells (AFC), Phosphoric Acid Fuel Cell (PAFC), Molten Carbonate Fuel Cell (MCFC) and Direct Methanol Fuel Cells (DMFC) [2][3]. One of these is considered the best due to its multiple advantages such as: delivers clean energy, a low operating temperature, a high overall efficiency in cogeneration (electricity and heat) up 60%, fast start-up. The PEM fuel cell occupies a wide space in several applications like mobile, residential, electric vehicle and space applications [4-6].

The energy produced by the PEMFC is closely related to a set of factors such as the partial gas pressure of hydrogen and oxygen, the stoichiometry, the cell temperature and the water membrane content (WMC) [7]. However, under constant operating conditions, we only find one point on the Power-Current curve, which shows the maximum power point (MPP), where the PEMFC system produces it's the maximum power. Hence, a MPP tracking (MPPT)

algorithm is wanted for the PEMFC system to raise the efficiency. In the In our study[8], we present a review of some representative studies on fuel cell MPPT in the last decade, in which has seen a huge development of the MPPT controller for fuel cell power systems, among them: Perturbation and Observation (P&O)[9], Incremental Conductance (IC) [10], Eagle Strategy (ES) [11], Extremum seeking control (ESC) [12], Fuzzy Logic Controller (FLC) [13], Particle Swarm Optimization (PSO) [14], Sliding Mode Control (SMC) [15], Artificial Neural Networks (ANN) [16], etc.

Power electronic interfacing circuit is called power conditioning unit. It is necessary for PEM Fuel Cell based systems to condition its output DC voltage. It converts the DC voltage to AC voltage. The FC source is connected to the load or grid through inverter which must be synchronized with the grid in terms of voltage and frequency (Fig. 1).

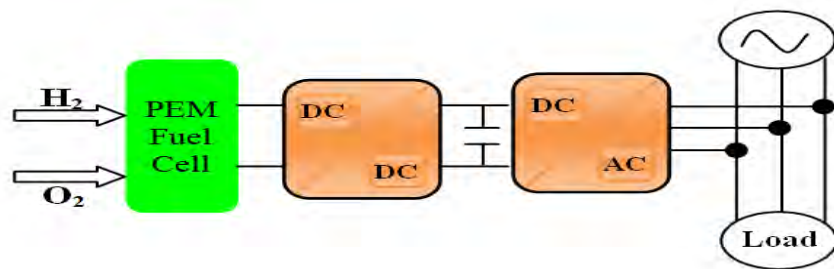


Fig. 1. Grid-connected fuel cell power system.

The major technical contributions of this paper are:

- . Enriching the literature with new technology by using stateflow chart for design the algorithm of MPPT and the inverter.
- . Reducing the response time, overshoot, oscillations around MPP and ripple.
- . Improvement the performance of PEMFC
- . Decreasing the fluctuations/disturbances allow increase the life of the PEMFC.
- . Showing the Vss IC MPPT as robust technique under variations operating conditions (temperature and water membrane content) compared to Fss IC MPPT.

The remaining of this paper is organized as follows: section 2 describes the PEM fuel cell modeling. The DC-DC boost converter, the MPPT control algorithm as well as the DC-AC

converter are presented in sections 3, 4 and 5, respectively. The main results and discussion are given in section 6. While section 7 gives the main conclusions are set out in giving some perspectives for future works.

2. Description and Modeling of PEM Fuel Cell

The overall chemical reaction in the fuel cell stack is located in each primary cell. Therefore, the primary cell requires several of basic constituents and has mechanical, chemical and electrical properties specific to ensure a good performance in the fuel cell stack. The polymer electrolyte membrane fuel cell particularly (PEMFC) is composed generally the principal elements following: electrolyte (membrane), electrodes (anode and cathode), diffusion layers and bipolar plates [17].

PEMFC is an electrochemical device that produces electricity, heat and water from two separated chemical reaction and this is done only by presence two chemical elements hydrogen and oxygen [18]. The hydrogen used as a fuel is introduced on the side of the anode, while oxygen as an oxidant is introduced on the side of the cathode (Fig. 2).

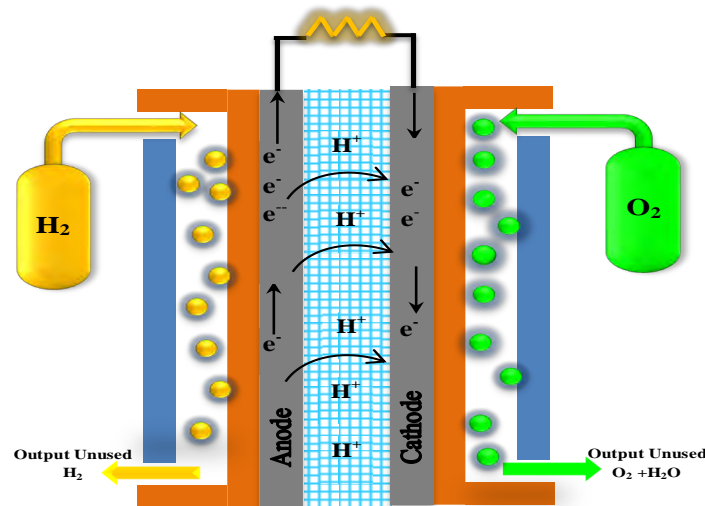


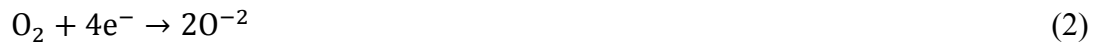
Fig. 2. PEM Fuel Cell.

The set of these Oxydo-Reduction reactions of hydrogen and oxygen respectively are illustrated below [19], [20]:

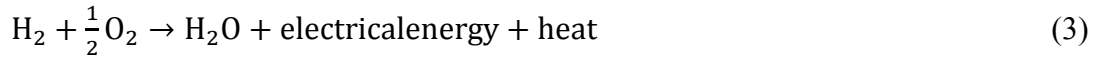
The half-reaction of oxidation of hydrogen will be as follows:



The half-reduction reduction of oxygen will be as follows:



The overall reaction taking place at the fuel cell can be summarized as:



Each cell voltage can be defined by the well-known expression given by [21]:

$$V_{\text{FC}} = E_{\text{Nernst}} - V_{\text{act}} - V_{\text{ohmic}} - V_{\text{conc}} \quad (4)$$

The output cell voltage which expressed by the equation of Nernst is expected to decrease even further as a function of current being provided, owing to unavoidable losses. There are three types of voltage losses inside PEMFC namely the activation, ohmic, and concentration voltage losses.

E_{Nernst} is the reversible open circuit voltage depending on temperature (T), oxygen pressure (P_{O_2}) and hydrogen pressure (P_{H_2}), in which approximated by [22]:

$$E_{\text{Nernst}} = 1.229 - (8.5 \times 10^{-4})(T - 298.15) + (4.385 \times 10^{-5}T[\ln(P_{\text{H}_2}) + 0.5\ln(P_{\text{O}_2})]) \quad (5)$$

V_{act} is the activation voltage drop occurs in anode and cathode, given by the Tafel equation [22], [23]:

$$V_{\text{act}} = \xi_1 + \xi_2 \cdot T + \xi_3 \cdot T \cdot \ln(C_{\text{O}_2}) + \xi_4 \cdot T \cdot \ln(i_{\text{FC}}) \quad (6)$$

where ξ_i ($i = 1$ to 4) are parametric coefficients for each cell; i_{FC} is the cell current and C_{O_2} is the oxygen's concentration defined by:

$$C_{\text{O}_2} = \frac{P_{\text{O}_2}}{(5.08 \times 10^6) \times \exp(-\frac{498}{T})} \quad (7)$$

V_{ohmic} is the ohmic linear voltage drop proportional to electric current, occurs due to the ionic resistance of the polymer membrane to the flow of protons as well as the resistance of the electrode materials and the bipolar plates resistance to the movement of electrons approximated by [24]:

$$V_{\text{ohmic}} = R_{\text{ohmic}} \cdot i_{\text{FC}} \quad (8)$$

where i_{FC} is the cell current; R_{ohmic} is the sum of the contact resistance R_c and the membrane resistance R_m considered defined by:

$$R_m = \frac{181.6 \times \left[1 + 0.03 \times \left(\frac{i_{FC}}{\delta} \right) + 0.062 \times \left(\frac{T}{303} \right)^2 \left(\frac{i_{FC}}{\delta} \right)^{2.5} \right]}{\left[\varphi - 0.634 - 3 \times \left(\frac{i_{FC}}{\delta} \right) \right] \exp \left(4.18 \times \left(T - \frac{303}{T} \right) \right)} \times \frac{\ell}{\delta} \quad (9)$$

where ℓ is the thickness of membrane (cm), δ is the cell active area (cm²) and φ is membrane water content.

V_{conc} is the concentration voltage drop from the transport of hydrogen and oxygen approximated by [25]:

$$V_{conc} = -\frac{RT}{\kappa F} \cdot \ln \left(1 - \frac{i_{FC}}{I_{max}} \right) \quad (10)$$

where R is universal gas constant, F is Faraday’s constant, κ is number of electrons participating in reaction and I_{max} is the maximum current density.

The parameters values of constants mentioned in the above equations are listed in Table 1

Table. 1 PEM fuel cell modeling parameters.

| Parameters | Value | Unit |
|------------|------------------------|-----------------|
| F | 96485.309 | C/mol |
| R | 8.3144 | J/mol K |
| ξ_1 | -0.9514 | V |
| ξ_2 | 3.12×10^{-3} | V/K |
| ξ_3 | 7.4×10^{-5} | V/K |
| ξ_4 | -18.7×10^{-5} | V/K |
| R_c | 0.0003 | Ω |
| ℓ | 0.0178 | Cm |
| δ | 16 | cm ² |
| κ | 2 | / |

By substituting all sides of equation 4 with their expressions into the equations 5, 6, 8 and 10, the characteristics curves (V-I) and (P-I) of the PEMFC are shown in Figures 3 and 4 were established for operating conditions constant at a temperature of 25°C and membrane water content equal to 14. Table 2 gives the parameters of the 5.5kW PEM fuel cell:

Table. 2 PEM Fuel Cell Parameters.

| Parameters | Value |
|--|-------|
| Maximum power at MPP (W) | 5500 |
| Cell open circuit voltage (V) | 1.29 |
| Number of cells | 500 |
| Cell active surface (cm ²) | 16 |
| Hydrogen partial pressure H ₂ (bar) | 2.6 |
| Oxygen partial pressure O ₂ (bar) | 0.3 |

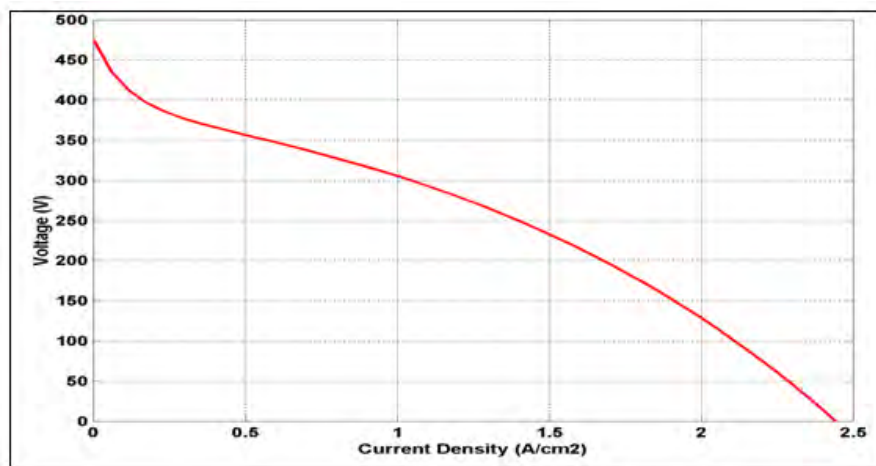


Fig. 3 5.5kW PEMFC V-I Characteristic.



Fig. 4 5.5kW PEMFC P-I Characteristic.

The characteristics curves of PEMFC voltage and power given in both Fig. 3 and Fig. 4, are nonlinear functions of PEMFC current, the power increases gradually to the maximum power point produced by this model and then decreases.

Fig. 5 and Fig. 6 present the characteristic (P-I) of the fuel cell system according to the variations of temperature and membrane water content, respectively. From these both characteristics the output power of the PEMFC is a nonlinear function of current and it is highly influenced by the operating conditions temperature and membrane water content. Each curve has a MPP at which the fuel cell array operates with the highest efficiency. Thus, the use of MPPT controller is necessary.

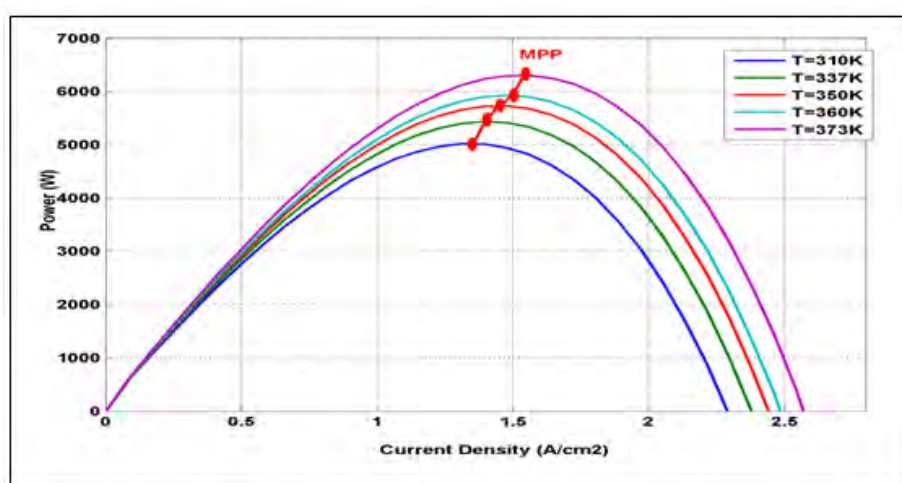


Fig. 5 5.5kW PEMFC P-I Characteristic under temperature variations.

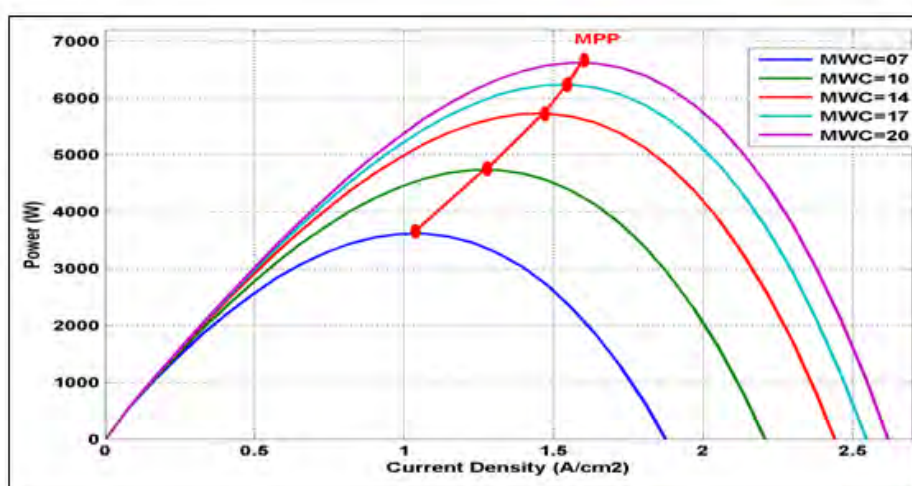


Fig. 6 5.5kW PEMFC P-I Characteristic under MWC variations.

3. DC-DC Boost Converter

The elevator chopper or boost converter is used as an interface between the photovoltaic generator and the inverter; their components are the inductances, capacitor, the diode and the thyristor (Fig. 7).

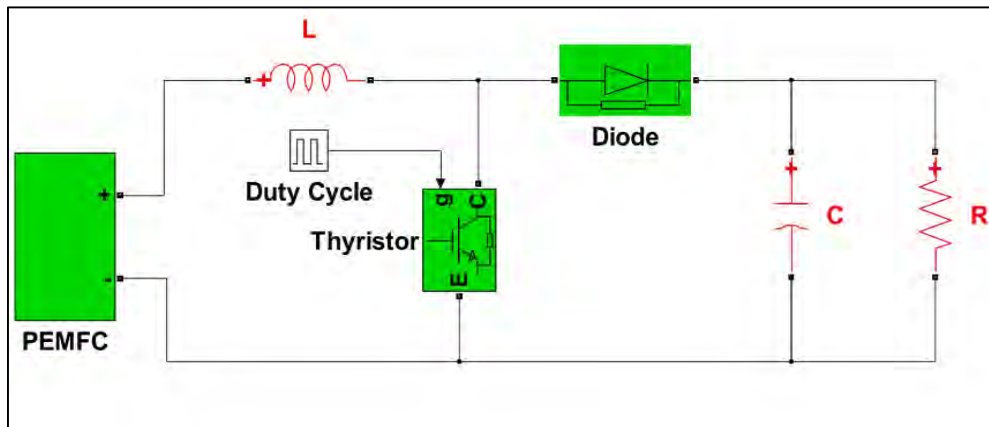


Fig. 7. DC-DC Boost converter.

Boost converter circuit operation can be divided into two phases according to the state of opening and closing of the thyristor as given in equation bellow:

$$\delta = \begin{cases} 0 & \text{Thyristor open} \\ 1 & \text{Thyristor closed} \end{cases} \quad (11)$$

The application of the Kirchhoff laws on the equivalent circuit of the Boost converter for a period of operation $[0-T_s]$, gives the following equation [25]:

$$\begin{cases} \frac{dV_{FC}}{dt} = \frac{1}{C_1} (i_{FC} - i_L) \\ \frac{di_L}{dt} = \frac{1}{L} (V_{FC} - (1 - \delta)V_{out}) \\ \frac{dV_{out}}{dt} = \frac{1}{C_2} ((1 - \delta)i_L - i_{out}) \end{cases} \quad (12)$$

where (i_{FC}, V_{FC}) and (i_{out}, V_{out}) are input and output current and voltage; respectively; i_L is the inductance current, C_1 , C_2 and L are capacitances and inductance values.

The output voltage is given as a function of the input voltage and the following duty cycle according to the following equation [26]:

$$V_{out} = \frac{V_{FC}}{1-D} \quad (13)$$

The capacitor and the inductor must be properly dimensioned to maintain a voltage at its terminals and current constant with a tolerated ripple.

$$L = \frac{V_{FC} \times D}{\Delta I_L \times F_s} \quad (14)$$

$$C = \frac{V_{out} \times D}{\Delta V_{out} \times F_s \times R_{Load}} \quad (15)$$

The simulations were performed on boost converter with the following parameter values mentioned in Table 3:

Table. 3 DC/DC Boost Converter Parameters.

| Parameters | Value |
|---------------------------------|-------|
| Inductor L (mH) | 2 |
| Capacitor C (μ F) | 200 |
| Switching frequency F_s (kHz) | 10 |

4. MPPT control algorithm

Several techniques have been developed to determine the MPP. In this simulation, a boost converter is used as a maximum power point tracker. The control signal is generated to control the switch state. The control circuit adjusts the duty cycle of the switch control waveform for maximum power point tracking. The variable step size incremental conductance MPPT controller is introduced for PEMFC to improve the drawbacks of the conventional fixed step size IC MPPT and represented in three points are: high oscillations around MPPT, slow dynamic response with overshoot and ripple [27].

The output current and voltage of the PEMFC are measured to calculate the conductance and the incremental conductance. The tracking MPP from the P-I characteristics correspond to the extent to which the relationship is achieved the derivative of PEMFC output power in relation to current [28]:

$$\frac{dP}{dI} = 0 \quad (16)$$

Equation (16) can be rewritten as:

$$\frac{dP}{dI} = \frac{d(I \times V)}{dI} = V + I \times \frac{dV}{dI} = 0 \tag{17}$$

$$\begin{cases} \frac{dV}{dI} = -\frac{V}{I} & \text{at MPP} \\ \frac{dV}{dI} > -\frac{V}{I} & \text{at left of MPP} \\ \frac{dV}{dI} < -\frac{V}{I} & \text{at right of MPP} \end{cases} \tag{18}$$

The Stateflow chart implementation of the IC MPPT is presented in Fig. 8

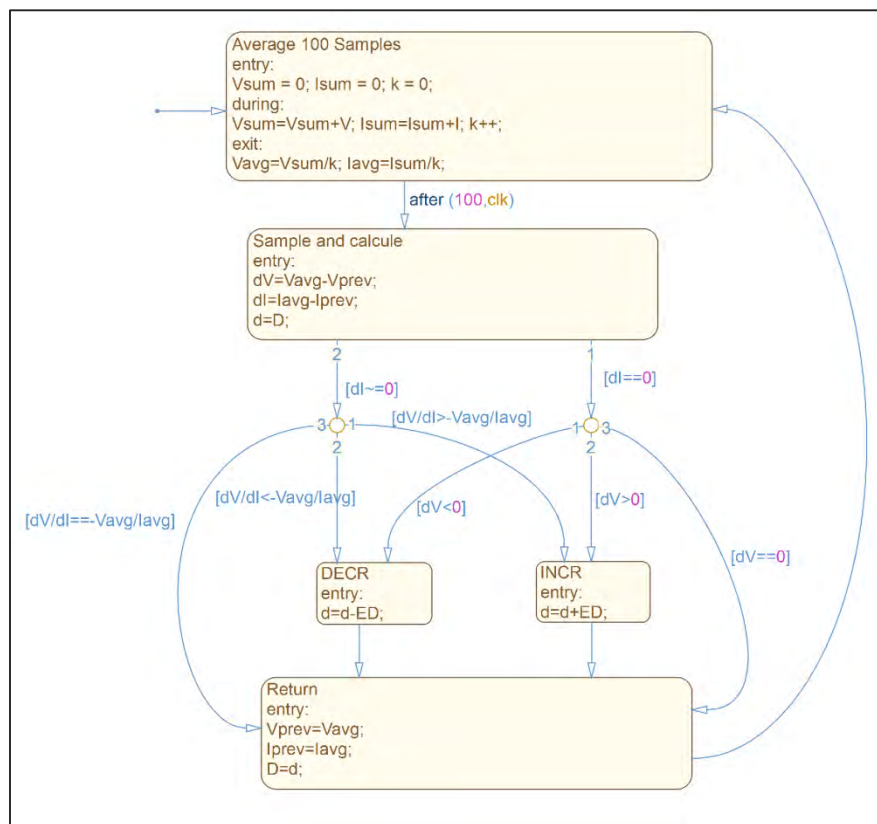


Fig. 8. Stateflow chart of the IC MPPT.

The calculation of the step size is given by:

$$D(k) = D(k - 1) \pm \alpha \cdot \left| \frac{dP}{dI} \right| \tag{19}$$

where D(k) and D(k-1) are the duty cycle at instants k and k-1; α is the fixed step size; dP and dI are power and current change.

The equation (19) implemented in Matlab using Stateflow chart is presented in Fig. 9

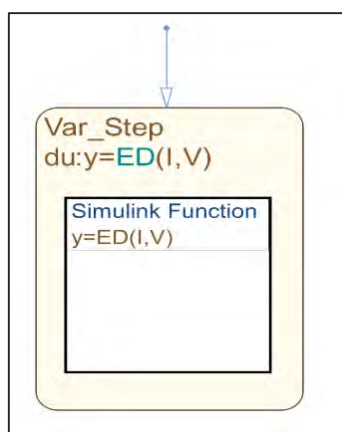


Fig. 9. State flow Equation (19).

5. DC-AC Converter

The role of the three-phase inverter is to pass the continuous electrical power to the grid. The output of the inverter can take three voltage levels depending on the DC source voltage and switch states. Voltage inverters can be controlled according to several strategies. At high frequency, they are controlled in pulse width modulation. Pulse width modulation (triangle sine) is realized by comparing a modulating low frequency bung (reference voltage) with a high frequency carrier wave of triangular form. The switching times are determined by the intersection points between the carrier and the modulator, the switching frequency of the switches is fixed by the carrier (Fig. 10).

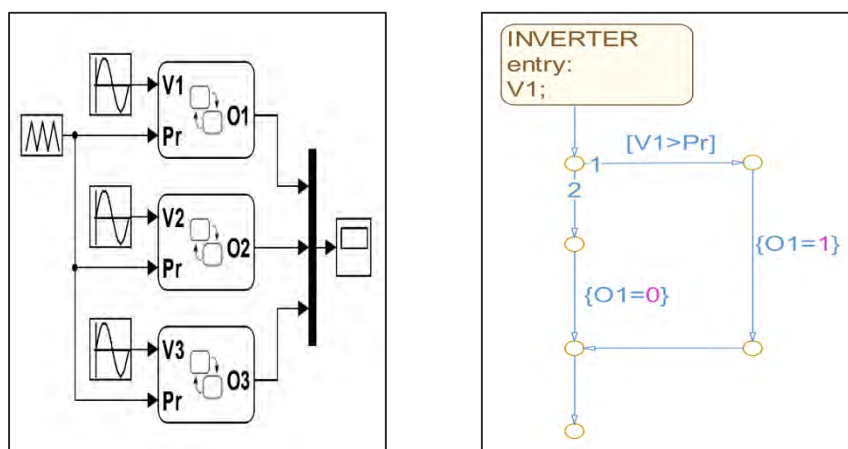


Fig. 10. State flow DC-AC.

6. Results and discussion

As first step in this simulation is the design of PEMFC by the determination of numbers of cell and the active area. The highest voltage of a PEMFC cell is approximately 0.5V and the current density is 1.4A/cm², this voltage and current density corresponds to the maximum power delivered by the PEM Fuel Cell. We have developed a fuel cell which has 500 numbers of fuel cells connected in series with active area about 16cm². This number of cells corresponds to five stacks connected in series, each stack is an assembly of 100 cells in series. The stack produced maximum power reaches 5.5kW, the output current; voltage and power are shown in Figures 11 to 13.

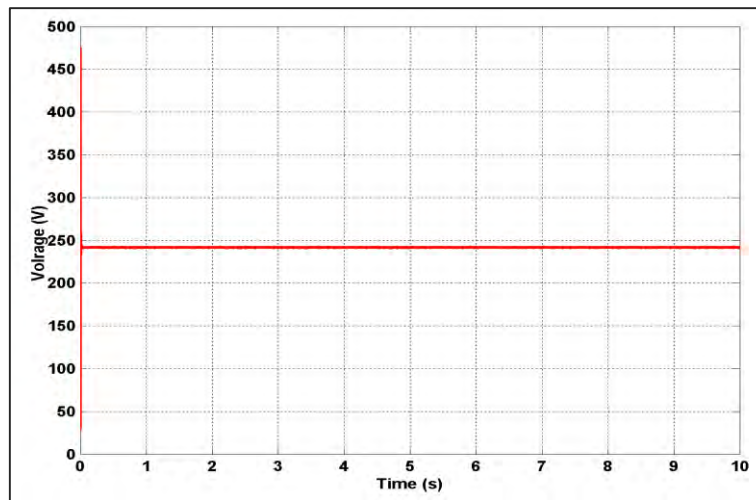


Fig. 11. Output Voltage.

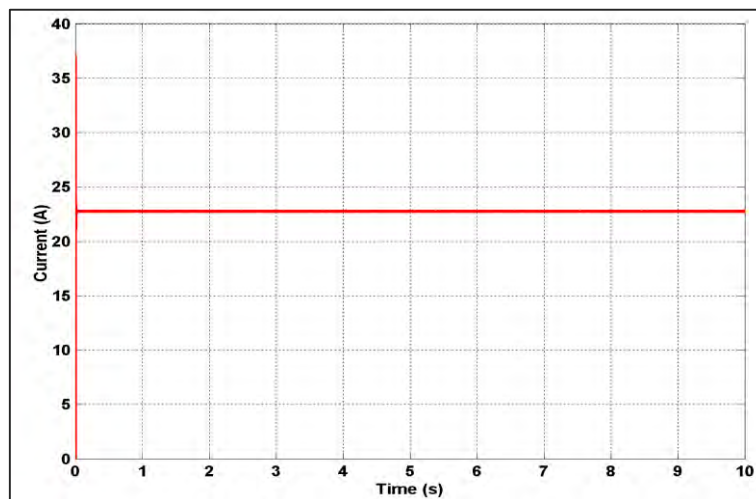


Fig. 12. Output Current.

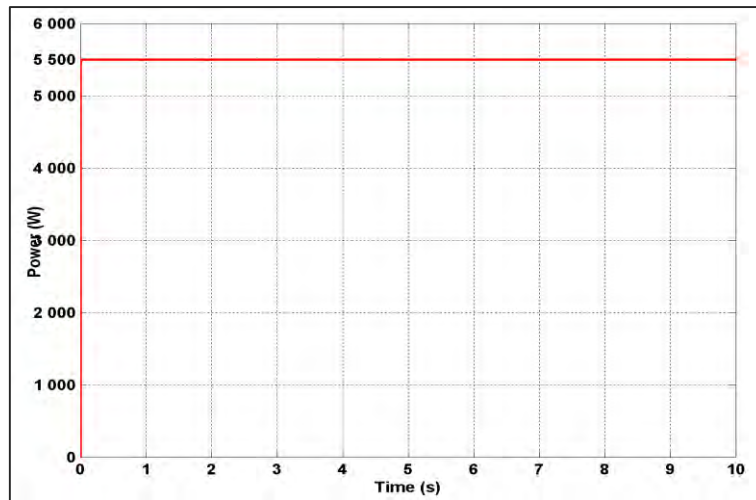


Fig. 13. Output Power.

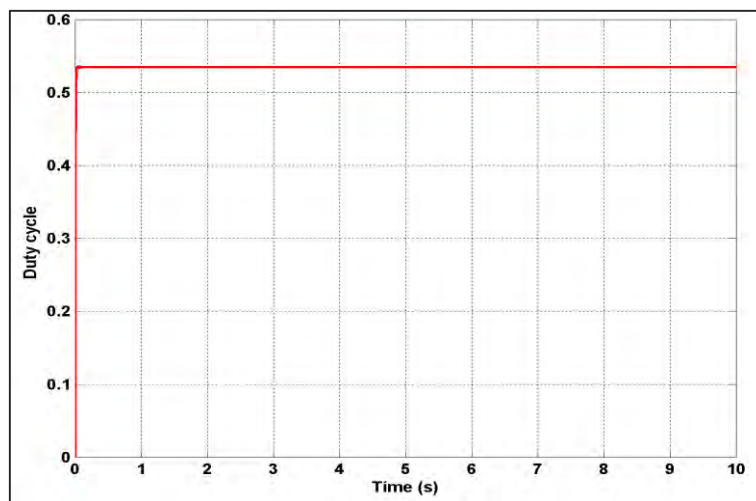


Fig. 14. Duty cycle value.

The output of PEMFC is fed to the two-level inverter via DC/DC boost converter. The boost converter output voltage is shown in Fig. 15 that provides approximately 520V, which controlled through IC variable step size MPPT to adjust the duty cycle (Fig.14); while the grid voltages is shown in Fig. 16 The inverter fed by DC bus whose voltage between its terminals approximately equal 520V. The technique pulse width modulation is used to controller the switches of inverter. The three delivered voltages take the closest shape that sinusoidal.

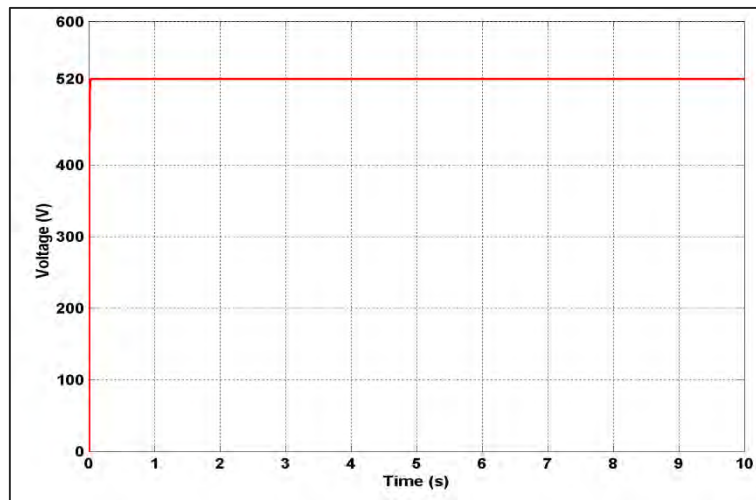


Fig. 15. Output Voltage of Boost Converter.

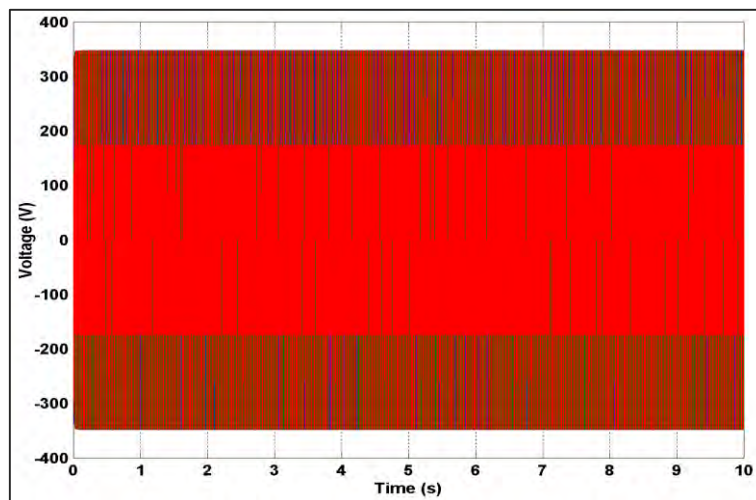


Fig. 16. Output Voltage of the two-level Inverter.

6.1 Case of temperature variations

Under constant pressure of H_2/O_2 and water membrane content, we evaluate in this part the different results of simulation with temperature changing as illustrated in Fig. 17.

Fig. 18 shows the output power using fixed step size (Fss) and variable step size (Vss) IC MPPTs in case of temperature variation. It is clearly that the operating temperature affected the PEMFC performance. Therefore, the PEMFC is sensitive to variation of temperatures and leads to improvement its performance when recording a rise in the operating temperature.

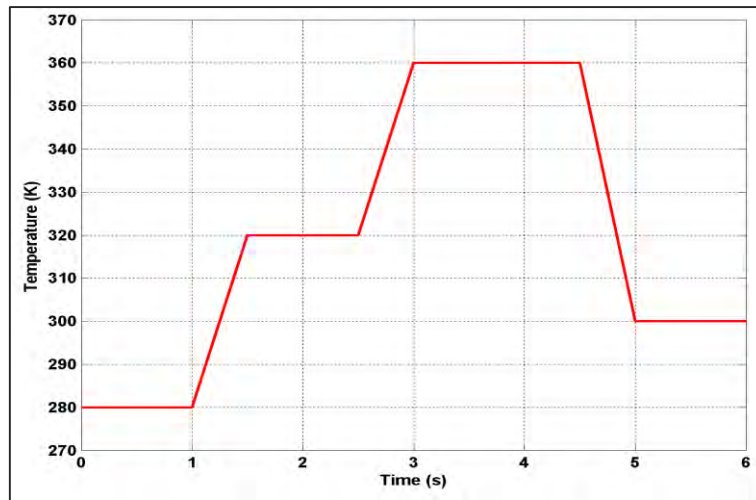


Fig. 17 Cell temperature variations.

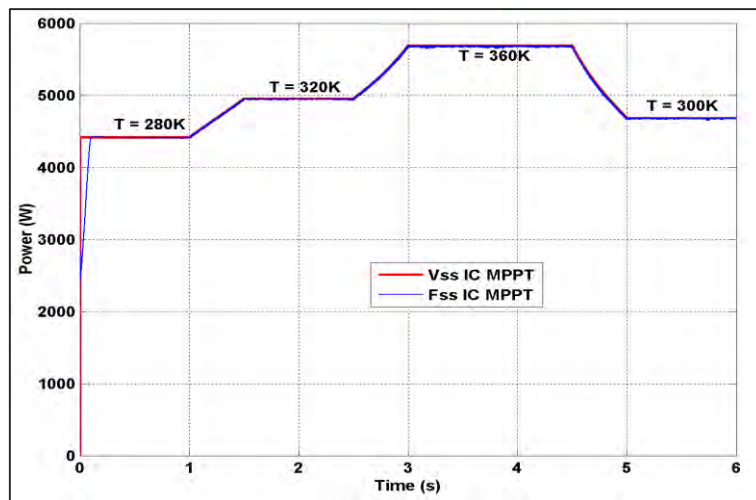


Fig. 18 PEMFC output power in case of cell temperature variation.

6.1.1 Dynamic performance in case of temperature variations

Fig. 19 present the output power from the interval 0-0.2s corresponding to $T=280K$. From this figure, we can see the algorithm Vss IC MPPT has good performance than Fss IC MPPT in terms of convergence time to reach the output power corresponding (4413w) with 0.004s for Vss IC MPPT instead of 0.1s for the Fss IC MPPT algorithm. In addition, the Vss IC MPPT presents one overshoot reach at 2381W compared to Fss IC MPPT presents two overshoot 2381W and 1947W before to stabilize.

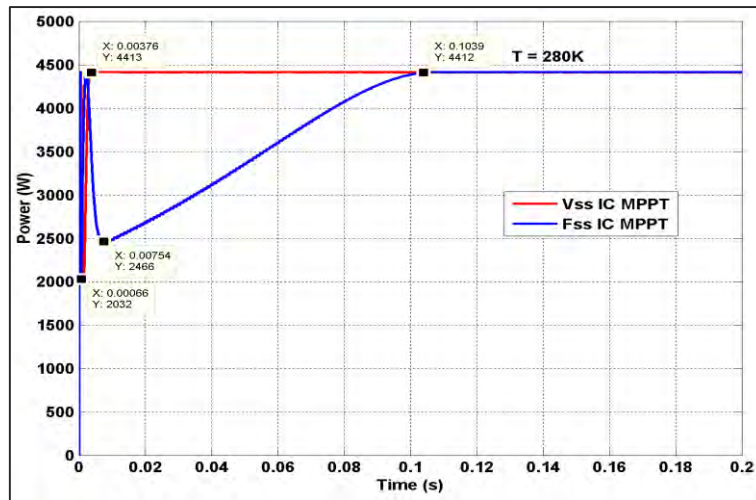


Fig. 19 Response time and overshoot of PEMFC output power for the interval 0-0.2s.

6.1.2 Static performance in case of temperature variations

Fig. 20 present the output power from the interval 1.8-1.82s corresponding to $T=320K$. The figure illustrates the ripple for both used algorithms. The algorithm Vss IC MPPT shows fewer ripples compared to the Fss IC MPPT; in which, we can see the ripple about the maximum power (4954W) reaches at its maximum 5w for Vss IC MPPT, while for Fss IC MPPT reaches at 18W.

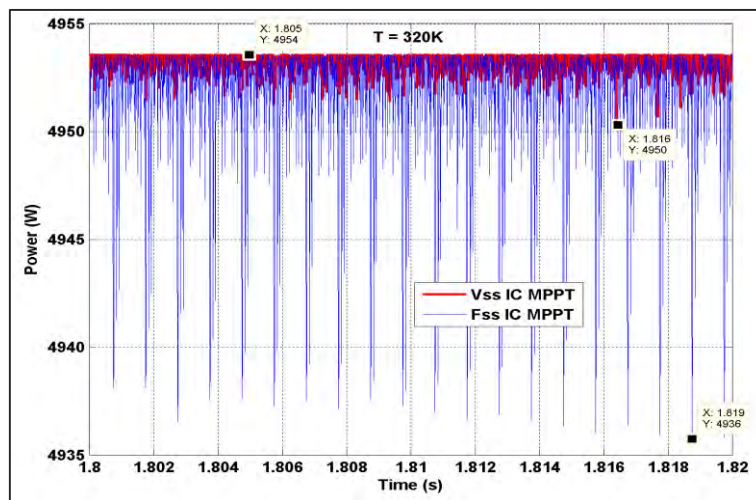


Fig. 20 The ripple of PEMFC output power for the interval 1.8-1.82s.

6.1.3 Output Voltage of Boost Converter and Inverter in case of temperature variations

Fig. 21 and Fig. 22 showed the output voltage of boost converter and the inverter in case of cell temperature variation respectively. From both figures, we can see clearly the effect of temperature variation, in which the voltage increased with raises of temperature.

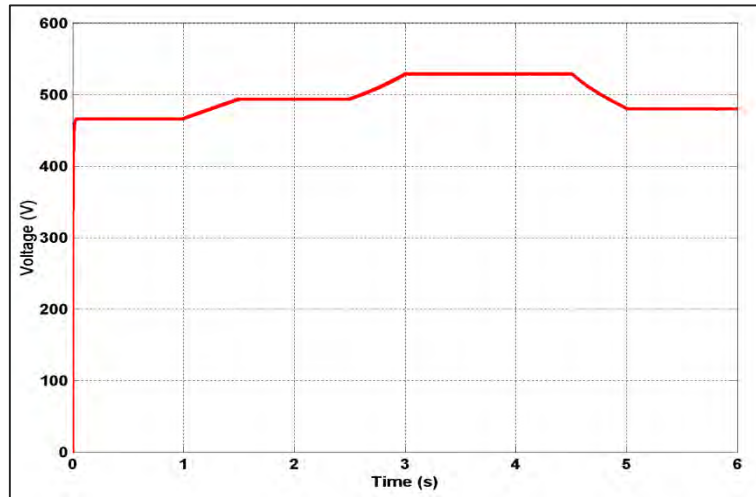


Fig. 21. Output Voltage of Boost Converter in case of cell temperature variation.

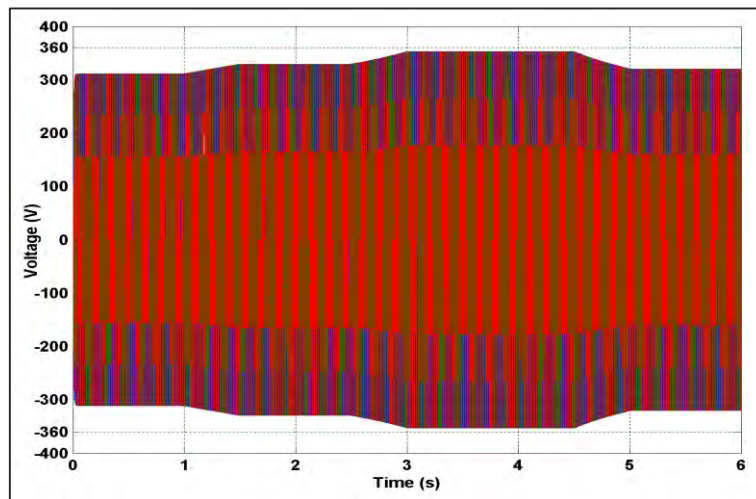


Fig. 22. Output Voltage of two-level Inverter in case of cell temperature variation.

6.2 Case of water membrane content variations

In this part, we change in the water membrane content value as illustrate in Fig. 23 with keeping both temperature and pressure constant to evaluate the tracking capability of the Vss IC MPPT controller.

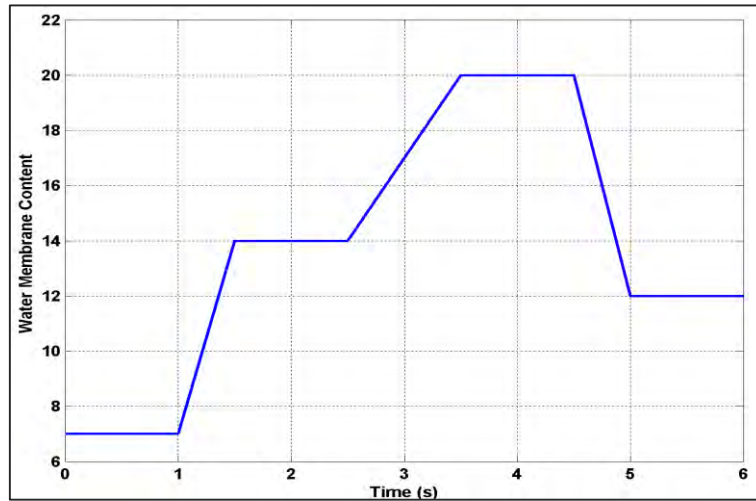


Fig. 23. Water Membrane Content variations.

Fig. 24 shows the corresponding output power.

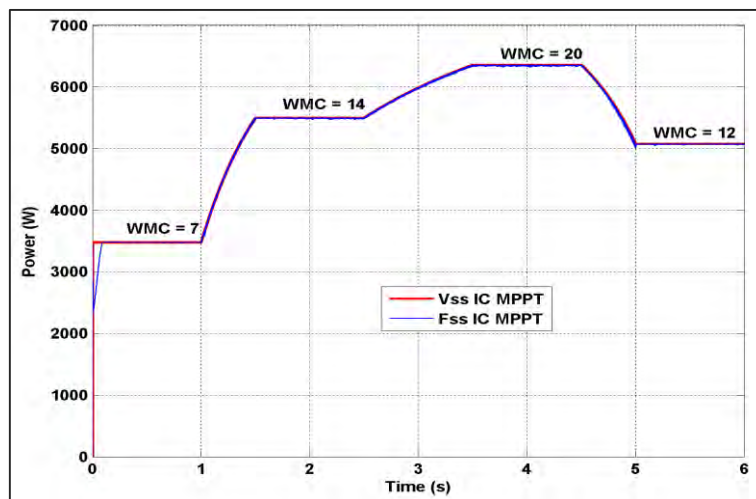


Fig. 24 PEMFC output power in case of Water Membrane Content variations.

Like changes of the operating temperature inside PEMFC, the variations of water membrane content affect the PEMFC performance as shown in Fig. 24. Therefore, the PEMFC performances increases or decreases dramatically with variation of the membrane water content. The rising of water membrane content will improve the maximum output power. When (WMC = 07), the corresponding maximum output power is 3479 W; while it increasing to reach 5500W at WMC = 14. In addition, from Fig. 24, similar as noticed in the case of temperature change, globally both MPPT controllers track the corresponding output power in case of membrane water content changing.

6.2.1 Dynamic performance in case of water membrane content variations

Fig. 25 present the output power from the interval 0-0.2s corresponding to WMC=7. From this figure, the algorithm Vss IC MPPT makes the PEMFC system deliver its maximum power in less time compared to the Fss IC MPPT algorithm. After 0.004s the PEMFC system with Vss IC MPPT reaches at its maximum power 3478W instead of 0.01s to reach the maximum output power corresponding 3478W with Fss IC MPPT. In addition, the Vss IC MPPT presents good performance in terms of overshoot compared to Fss IC MPPT.

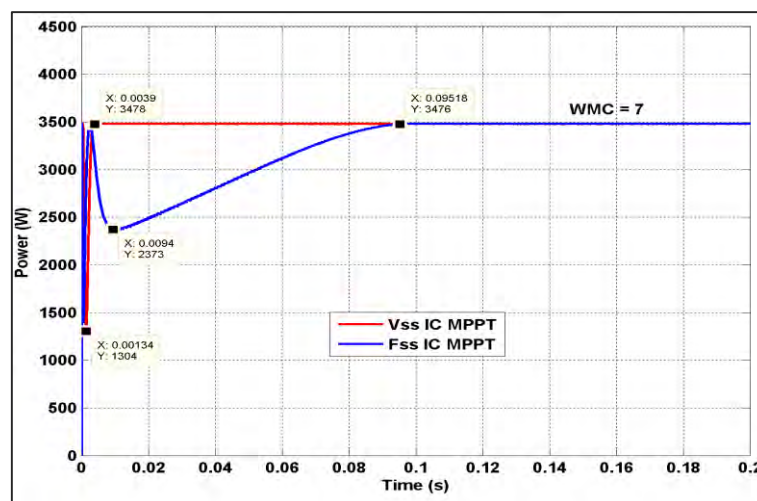


Fig. 25 Response time and overshoot of PEMFC output power for the interval 0-0.2s.

6.2.2 Static performance in case of water membrane content variations

Similarly to the case of temperature change, the generated ripple with Fss IC MPPT algorithm under water membrane content change is higher than Vss IC MPPT as presented in Fig. 26. From figure, we can see the ripple about the maximum power (5503W) reaches at its maximum 5w for Vss IC MPPT, while for Fss IC MPPT reaches at 24W.

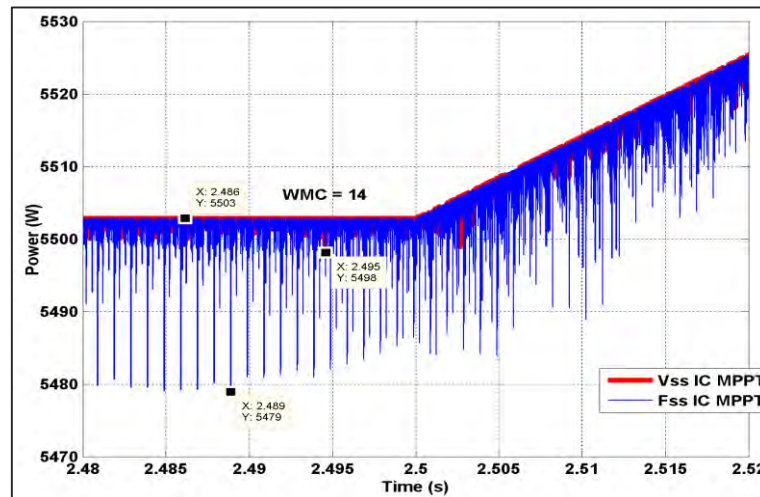


Fig. 26 The ripple of PEMFC output power for the interval 2.48-2.52s.

6.2.3 Output Voltage of Boost Converter and Inverter in case of water membrane content variations

Fig. 27 and Fig. 28 showed the output voltage of boost converter and the inverter in case of water membrane content variations respectively. From both figures, we can see clearly the effect of water membrane content variations, in which the voltage increased with raises of temperature.

7. Conclusions

The PEMFC stack is developed in this studied using DC/DC boost converter with two-level inverter and power system parameters. This model would be useful to define the structure of grid connected environment. The IC variable step size MPPT is used for controlling the duty

cycle in order to maintain the PEMFC stack operating at its maximum power and delivered the desired DC voltage that would feed the grid through inverter after conversion. The PWM is adopted to deliver the switching pulses of the DC/AC inverter. These controllers facilitate developing a fuel cell based power conditioning system so that PEMFC stack can be connected to any grid for meeting power requirements.

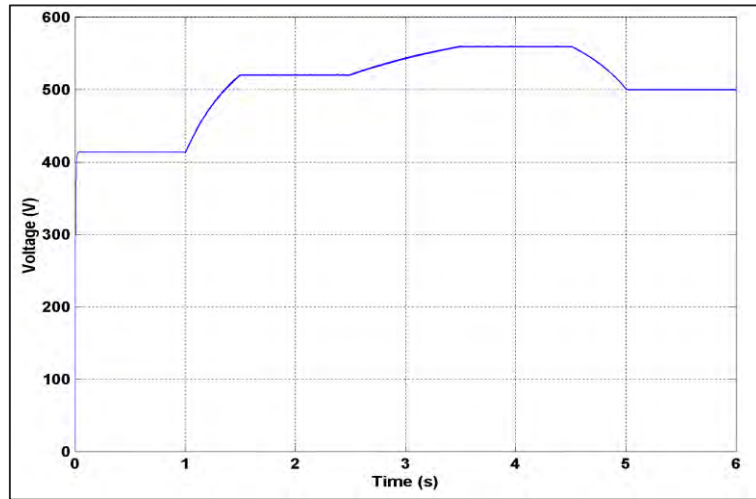


Fig. 27. Output Voltage of Boost Converter in case of WMC variations.

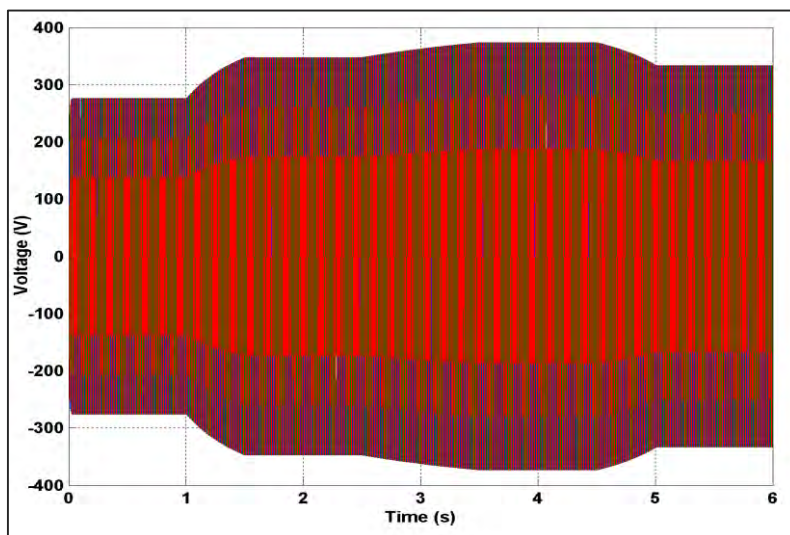


Fig. 28. Output Voltage of two-level Inverter in case of WMC variations.

8. Acknowledgements

The Algerian Ministry of Higher Education and Scientific Research via the DGRSDT supported this research (PRFU Project code: A01L07UN190120180005).

9. References

- [1] Chae, K.J., Kim, I.S., Ren, X., Cheon, K.H., Reliable energy recovery in an existing municipal wastewater treatment plant with a flow-variable micro-hydropower system. *Energy Convers Manag* 2015;101:681–8. doi:10.1016/j.enconman.2015.06.016.
- [2] Mostafaeipour, A., Qolipour, M., Rezaei, M. and Babae-Tirkolae, E., Investigation of off-grid photovoltaic systems for a reverse osmosis desalination system: A case study, *Desalination*, 454, pp. 91-103 (2019).
- [3] Mekhilef, S., Saidur, R. and Safari, A., Comparative study of different fuel cell technologies, *Renewable and Sustainable Energy Reviews*, 16, pp. 981-989 (2012).
- [4] Inci, M. and Türksoy, O., Review of fuel cells to grid interface: Configurations, technical challenges and trends, *Journal of Cleaner Production*, 213, pp. 1353-1370 (2019).
- [5] Abderezzak, B., Rekioua, D., Binns, R., Busawon, K., Hinaje, M., Douine, B. and Guilbert, D., Technical feasibility assessment of a PEM fuel cell refrigerator system, *International Journal of Hydrogen Energy*, pp. 1-9 (2018).
- [6] Sankar, K. and Jana, A.K., Nonlinear multivariable sliding mode control of a reversible PEM fuel cell integrated system, *Energy Conversion and Management*, 171, pp. 541-565 (2018).
- [7] Wang, T., Qi, Li, Yin, L. and Chen, W., Hydrogen consumption minimization method based on the online identification for multi-stack PEMFCs system, *International Journal of Hydrogen Energy*, 44, pp. 5074-5081 (2019).
- [8] Harrag, A., Bahri, H., A Novel Single Sensor Variable Step Size Maximum Power Point Tracking for Proton Exchange Membrane Fuel Cell Power System, *Fuel Cells* 19 (2), 177-189.
- [9] Romdlony, M.Z., Trilaksono, B.R., Ortega, R, Experimental study of extremum seeking control for maximum power point tracking of PEM fuel cell. In: *International Conference on System Engineering and Technology (ICSET)*; 2012. p. 1e6.

- [10] Harrag, A., Messalti, S., Variable step size IC MPPT controller for PEMFC power system improving static and dynamic performances, *Fuel Cells* 17 (6), 816-824
- [11] Sarvi, M, Parpaei, M, Soltani, I, Taghikhani, M.A, Eagle strategy based maximum power point tracker for fuel cell system. *IJE Trans A Basics* 2015;28(4):529e36.
- [12] Jiao, J, Cui, XA. Real-time tracking control of fuel cell power systems for maximum power point. *J Comput Inf Syst* 2013;9(5):1933e41.
- [13] Harrag, A., Messalti, S., How fuzzy logic can improve PEM fuel cell MPPT performances, *International Journal on Hydrogen Energy*, 43, 2018:537-550.
- [14] Soltani, I, Sarvi, M, Marefatjou, H, An intelligent, fast and robust maximum power point tracking for proton exchange membrane fuel cell. *World Appl Program* 2013;3(7):264e81.
- [15] Silaa, M.Y., Derbeli, M., Barambones, O., Cheknane, A., Design and Implementation of High Order Sliding Mode Control for PEMFC Power System, *Energies* 2020, 13(17), 4317.
- [16] Harrag A, Bahri H, Novel neural network IC-based variable step size fuel cell MPPT controller, *Int. Journal of Hydrogen Energy*, 42(5), 2017:3549-3563.
- [17] Wu, H.W., A review of recent development: Transport and performance modeling of PEM fuel cells, *Applied Energy*, 165, pp. 81-106 (2016).
- [18] Wang, C., Nehrir, M.H., Shaw, S.R., Dynamic models and model validation for PEMFC using electrical circuits, *IEEE Trans Energy Convers*, 20(2), pp. 442-451 (2005).
- [19] Beicha, A., Modeling and simulation of proton exchange membrane fuel cell systems'' *Journal of Power Sources*, 205, pp. 335–339 (2012).
- [20] Sun, Z., Wang, N., Bi, Y. and Srinivasan, D., Parameter identification of PEMFC model based on hybrid adaptive differential evolution algorithm, *Energy*, 90, pp. 1334-1341 (2015).
- [21] Harrag, A. and Bahri, H. Novel neural network IC-based variable step size fuel cell MPPT controller Performance, efficiency and lifetime improvement, *International Journal of Engineering*, 42, pp. 3549-3563 (2017).
- [22] Bigdeli, N., Optimal management of hybrid PV/fuel cell/battery power system: A comparison of optimal hybrid approaches, *Renewable and Sustainable Energy Reviews*, 42, pp.377-393 (2015).
- [23] Seyezhai, R., Mathur, B.L., Modeling and control of a PEM fuel cell based hybrid multilevel inverter, *International Journal of Hydrogen Energy*, 36, pp.15029-15043 (2011).
- [24] Wang, Y.X., Yu, D.H., Chen, S.A., Kim, Y.B., Robust DC/DC converter control for polymer electrolyte membrane fuel cell application, *Journal of Power Sources*, 261, pp.292-305 (2014).

- [25] Chang, K.Y., The optimal design for PEMFC modeling based on Taguchi method and genetic algorithm neural networks, *International Journal of Hydrogen Energy*, 36, pp.13683-3694 (2011).
- [26] Coronado-Mendoza, A., Bernal-Agustín, J.L., Domínguez-Navarro, J.A., Photovoltaic boost converter system with dynamic phasors modeling” *Electric Power Systems Research*, 81, pp. 1840-1848 (2011).
- [27] Mirbagheri, S.Z., Mekhilef, S. and Mirhassani, S. M., MPPT with Inc.Cond method using conventional interleaved boost converter, *Energy Procedia*, 42, pp. 24–32 (2013).
- [28] Harrag, A. and Messalti, S., Variable Step Size IC MPPT Controller for PEMFC Power System Improving Static and Dynamic Performances, *Fuel Cells*, 17(6), pp. 816-824 (2017).
- [29] Karami, N., El Khoury, L., Khoury, G., Moubayed, N., Comparative Study Between P&O and Incremental Conductance for Fuel Cell MPPT, In: 2nd renewable energy of developing countries (REDEC), pp. 17-22 (2014).